Journal of Manufacturing Processes 134 (2025) 135–145

Contents lists available at ScienceDirect

Journal of Manufacturing Processes

journal homepage: www.elsevier.com/locate/manpro

Expanding the applicability of material jetting–printed photopolymer prototype injection moulds by gamma irradiation post-treatment

Szabolcs Krizsma [a], László Mészáros [a,b,*], Norbert Krisztián Kovács [a], András Suplicz [a,c]

[a] Department of Polymer Engineering, Faculty of Mechanical Engineering, Budapest University of Technology and Economics, Műegyetem rkp. 3, H-1111 Budapest, Hungary
[b] HUN-REN-BME Research Group for Composite Science and Technology, Műegyetem rkp. 3, H-1111 Budapest, Hungary
[c] MTA-BME Lendület Lightweight Polymer Composites Research Group, Műegyetem rkp. 3, H-1111 Budapest, Hungary

ARTICLE INFO

Keywords:
Rapid tooling
Injection moulding
Material jetting
High-energy gamma irradiation
Dynamic mechanical analysis
Creep test

ABSTRACT

Additive manufacturing (AM) revolutionized modern production and tooling, as it can help speed up the development process. This is also true for injection moulding. For instance, polymeric low-volume injection moulds are easy to produce by material jetting (MJ) technologies like PolyJet™. The downside of these MJ printed moulds is their relatively low glass transition temperature, which can result in unacceptably low stiffness and increased creep compliance in the operational temperature range. Different post-curing techniques like high-energy irradiation can enhance the degree of cross-linking in MJ-printed photopolymer parts. We applied MJ (PolyJet™ technology) to produce specimens for mechanical and morphological characterizations and low-volume injection moulds. After printing, we subjected the specimens and the inserts to high-energy gamma irradiation with doses of 50 kGy, 100 kGy, 150 kGy and 200 kGy. Dynamic mechanical analysis (DMA) showed the effects of irradiation on material properties: the glass transition temperature of the photopolymer rose by almost 10 °C from 70.8 °C of the untreated insert to 81.6 °C of the specimen irradiated with 200 kGy. The creep time temperature superposition (TTS) tests proved that the increasing irradiation doses significantly reduced creep compliance, which resulted in considerably lower mould insert deformations. Creep compliance measured at 35 °C fell from 1920 $\mu m^2/N$ of the untreated specimen to 518 $\mu m^2/N$ of the specimen irradiated with 200 kGy. After the material tests, we applied an elaborated comprehensive state monitoring system (operational strain, cavity pressure and temperature measurements) to highlight the fundamental effect that the irradiation has on the operational behaviour of the MJ-printed mould inserts. Injection moulding tests showed that the increasing irradiation doses resulted in significantly decreased operational deformations. Maximal operational strain of the mould inserts fell from 1 % measured on the untreated (0 kGy) insert to 0.5 % measured on the insert irradiated with 200 kGy. It is highly desirable because product dimensional accuracy is also increased. Irradiation also significantly increased mould life (the number of products that can be manufactured), which is a crucial advantage from an economic point of view. We proved that post-curing by gamma radiation is a feasible way to enhance the applicability and the dimensional stability of photopolymer injection mould inserts. This is a definitely novel way to enhance the applicability of MJ-printed low-volume injection moulds.

* Corresponding author at: Department of Polymer Engineering, Faculty of Mechanical Engineering, Budapest University of Technology and Economics, Műegyetem rkp. 3, H-1111 Budapest, Hungary.
E-mail address: meszaros@pt.bme.hu (L. Mészáros).

https://doi.org/10.1016/j.jmapro.2024.12.037
Received 13 September 2023; Received in revised form 3 November 2024; Accepted 17 December 2024
Available online 27 December 2024

Nomenclature

Table 1
List of abbreviations and nomenclatures.

Abbreviation	Nomenclature
AM	Additive manufacturing
BCN	Carbon-doped boron nitride
CNT	Carbon nanotube
DLP	Digital light procession
DMA	Dynamic mechanical analysis
DMLS	Direct metal laser sintering
MFR	Melt flow rate
MJ	Material jetting
PEGDMA	Polyethylene glycol dimethacrylate
RT	Rapid tooling
TTS	Time temperature superposition

1. Introduction

Additive manufacturing (AM) has already made an impact on modern injection moulding industry. Additive technologies like material jetting (MJ) can produce nearly final and dimensionally accurate geometries in a single technological step. AM can also produce complicated, freeform geometries with undercuts or complex infill patterns that would otherwise be difficult or impossible to make with conventional technologies [1]. The combination of well-established manufacturing processes like injection moulding with AM leads to many new and much anticipated results. Polymeric additive technologies like MJ can produce low-volume injection moulds fast and cost-effectively. This combined technology is a fast-evolving field of rapid tooling (RT).

The international research community has already started to analyse the applicability of MJ printed mould inserts. An excellent example of this is the study of Zink et al. [2]. They printed mould inserts by PolyJet™ from FullCure720 and Digital ABS Plus (RGD5160-DM) photopolymer resins and applied different conformal cooling channel layouts to increase the cooling efficiency of the inserts. Their results showed that conformal cooling can reduce the heat load of the mould inserts by 70 % compared to the uncooled inserts. This way the lifetime of the inserts can be increased substantially. Mendible et al. [3] compared a PolyJet™ printed DigitalABS insert with a machined insert and a mould insert produced by direct metal laser sintering (DMLS). The metal inserts endured 500 injection moulding cycles and the PolyJet™ insert failed after 116 cycles. Bagalkot et al. [4] printed DigitalABS injection moulds and created an algorithm to set the injection moulding parameters to achieve maximal mould insert lifetime. They identified mould temperature, injection pressure, injection speed, holding pressure and cooling time as the critical processing parameters that determine mould lifetime. Simpson et al. [5] injection moulded using a steel mould (P20 tool steel) a DigitalABS mould and a FullCure720 mould. They found that the suitable injection moulding materials had the lowest possible melt temperature and required injection pressure. The parts injection moulded with the DigitalABS and FullCure720 moulds showed considerably lower flexural stiffness than the parts made with the steel mould. Davoudinejad et al. [6] used vat photopolymerisation to print mould inserts for micro-injection moulding from a methacrylic photopolymer resin. They subjected four inserts to thermal aging (keeping them at 100 °C and 23 °C, cyclically) and left two inserts in as-printed state. Failure occurred earlier for the aged inserts (between 35 and 110 cycles), while the unaged inserts cracked after 110 and 143 cycles. Davoudinejad et al. [7] created another case study with the above-mentioned mould insert where they reached failure cycle numbers ranging from 25 to 143 cycles. The lifetime of the inserts was heavily dependent on melt temperature, injection speed, mould temperature and cooling time. It can be generally concluded that polymeric inserts are sensitive to the thermal and mechanical loads occurring during injection moulding. Therefore, it is essential to keep melt temperature and the pressure load as low as possible. The lifetime of polymeric moulds can also be enhanced by keeping a long residual cooling time in the cycles and a long idle time between the cycles, which can retain the operational temperature of the mould inserts in an acceptable range.

The major downside of these polymeric moulds is their low strength and stiffness, the temperature dependence of the modulus of elasticity and their tendency to creep, especially at higher temperatures. Elkaseer et al. [8] concluded that UV-curable resins are easy to print by MJ and the products are dimensionally accurate. A main shortcoming is the relatively low mechanical and thermal performance of the printable materials. The relatively low T_g of epoxy-acrylate thermosets can be increased by introducing additional curing systems [9]. Golhin et al. [10,11] analysed the optical and appearance properties of MJ printed parts. They found that the surface texture of MJ printed parts is heavily influenced by the build orientation. Golhin et al. [12] also analysed the effect of accelerated aging (using cyclic UV-A irradiation) on the modulus of elasticity and T_g of PolyJet printed parts. They found that modulus of elasticity increased by up to 49 % while the glass transition temperature increased by 15 %. The mechanical properties of UV-curable resins are also heavily dependent on the curing parameters, such as the intensity of the UV light and the number of curing passes [13,14]. Zhao et al. [15] modelled the effect of UV irradiation on product properties. Their model considers the effect of processing parameters (UV source pathway, intensity, spatial distribution and interlayer attenuation) to optimize the printing process. The curing properties of polymers are also analysed when printing with vat photopolymerisation or material extrusion [16–19]. Limited mechanical strength and stiffness can be improved by different post-curing techniques. One of these is the application of ionizing radiation, like gamma irradiation. This kind of post-curing leads to two concurring phenomena. One is the increased cross-link density of the molecular chains, the other is chain scission. Cross-linking is dominant for photopolymers containing acrylate. The increase in cross-link density results in significantly higher modulus of elasticity, strength and hardness. It also increases the glass transition temperature, meaning that stiffness and strength only decrease drastically at higher temperatures [20,21]. The absorbed dose has an optimum as large doses of radiation lead to excessive chain scission and the degradation of the material [22–25].

Jiao et al. [26] subjected neat epoxy and carbon-doped boron nitride (BCN) composites with an epoxy matrix to gamma radiation. An irradiation dose in the range of 300–600 kGy enhanced the tensile strength of the neat epoxy and the epoxy–BCN composites by 5–20 %. Chen et al. [27] also applied gamma irradiation (from a ^{60}Co source) on epoxy resins. They subjected tensile specimens to 200, 500, 1000 and 2000 kGy doses with a dose rate of 100 Gy/min. After irradiation, the samples were subjected to physical aging at room temperature for a minimum of three months. The flexural strength and flexural modulus of the specimens increased significantly by the higher absorbed doses. Flexural strength rose from 110 MPa of the neat epoxy to 130 MPa of the sample irradiated by 2000 kGy. Flexural modulus also rose from approximately 2.9 GPa of non-irradiated epoxy to above 3.5 GPa of specimens irradiated with 2000 kGy. Wang et al. [28] used digital light procession (DLP) and printed samples using a photosensitive resin, which is a mixture of epoxy acrylate, PEGDMA (Polyethylene glycol dimethacrylate), and epoxy. The epoxy acrylate and the PEGDMA were cross-linked by UV light while the epoxy was cross-linked primarily by gamma radiation. The specimens were post-cured with the UV light for different time intervals (0 min, 2 min, 5 min, 10 min, 20 min, 40 min, 60 min and 90 min) and the post-cured specimens were then irradiated with different doses of gamma rays (0 kGy, 10 kGy, 100 kGy, 1000 kGy). They also used a ^{60}Co source to generate the gamma rays. The glass transition temperature and the storage modulus of the different samples were determined by DMA. Specimens that were not post-cured with the UV

light showed significantly higher T_g, ranging from 50.3 °C (0 kGy) to 71.5 °C (1000 kGy). The storage modulus of these specimens grew from 525 MPa (0 kGy) to 2530 MPa (1000 kGy). The increase in post-curing time also increased both T_g and the storage modulus at a given gamma radiation level from 0 kGy to 100 kGy. The T_g of the neat specimens (0 kGy gamma radiation) increased from 50.3 °C to 65.7 °C with increasing UV post-curing time. However, in the case of the 1000 kGy dose, a higher UV post-curing time tends to result in lower T_g and storage modulus, which can be caused by the over-curing of the system. Jiao et al. [29] analysed the effect of gamma radiation (^{60}Co source) on an epoxy resin and an epoxy resin with hexagonal boron nitride (h-BN). They found that the tensile strength of the neat epoxy and the epoxy–h-BN composites increased by approximately 15 % at an absorbed dose of 282 kGy, which is caused by radiation-induced cross-linking. With higher absorbed doses, chain scission and degradation becomes dominant, which results in a sharp decrease in tensile strength. Therefore, it is essential to use a suitably low dose, where degradation can be avoided. Hassan et al. [30] analysed the effect of gamma radiation on epoxy–tungsten boride composites. They irradiated the specimens with doses of 1000 kGy, 1500 kGy and 2000 kGy. The stress at break grew from 57.2 MPa of the non-irradiated specimen to 93.7 MPa of the specimen irradiated with 1000 kGy. Stress at break of the specimen irradiated with 2000 kGy was 80.2 MPa, which also highlights that a suitable dose has to be found where radiation-induced cross-linking can occur but chain scission is not dominant. Szebényi et al. [31] analysed the effect of gamma radiation on an epoxy resin, an epoxy–vinyl ester hybrid resin and these resin systems with carbon nanotube (CNT) reinforcement. They analysed four different doses (25 kGy, 50 kGy, 75 kGy and 100 kGy) and carried out three-point bending tests. A dose of 25 kGy significantly increased the bending modulus and bending strength compared to the non-irradiated specimens. An increase from 25 kGy did not increase the bending modulus and strength significantly. On the other hand, the deformation at break of the irradiated specimens decreased significantly compared to the non-irradiated specimens. Adhesion improved between the matrix material and the CNT. According to the above-mentioned studies, there is a fair chance of post-curing and enhanced mechanical properties in the 50–200 kGy absorbed dose range.

The already available research results suggest that ionizing radiation can help increase the durability of MJ-printed photopolymer prototype moulds and inserts. It is promising, because there is an ever-growing demand from the injection moulding industry for more durable prototype moulds and inserts. The underlying phenomenon is already known from material science but the application of irradiation to increase stiffness, strength and preserve them even at elevated temperatures is novel. In the present article, we performed in-depth material testing to find the optimal irradiation dose and to prove the beneficial effects of radiation on mechanical strength and stiffness. After material testing, the MJ printed injection mould inserts were subjected to gamma irradiation and the injection moulding series were carried out.

2. Materials and methods

2.1. Preparation of the samples

Rectangular specimens were printed for dynamic mechanical analysis with the dimensions of 4 × 10 × 59 mm. The specimens and the mould inserts were printed with an Objet Alaris 30 printer (Stratasys Ltd.) from an UV curable resin RGD835 (VeroWhite). The specimens were printed at room temperature (23 °C) in approximately 50 % relative humidity. The material is suitable for mould inserts because it has acceptable strength, stiffness and hardness. A significant limitation for its application is its relatively low glass transition temperature and low thermal conductivity, which results in slower heat extraction from the insert. Table 2 shows the material properties of RGD 835.

The radiation treatment of the specimens and printed moulds was carried out at the Institute of Isotopes Ltd. (Budapest, Hungary), with a panoramic SLL-01 type ^{60}Co radiation source. The dose rate was 2 kGy/h in all cases and the applied doses were the following: 50, 100, 150, and 200 kGy.

Table 2
Material properties of RGD 835 (VeroWhite).

Properties	Unit	Typical value
Tensile strength	MPa	50–65
Modulus of elasticity	GPa	2–3
Elongation at break	%	10–25
Flexural strength	MPa	75–110
Glass transition temperature	°C	52–54
Thermal conductivity	W/(m·K)	0.2
Coefficient of thermal expansion	1/K	$75 \cdot 10^{-6}$

2.2. Material testing

After the specimens were irradiated, they were analysed with a TA Instruments (USA) Q800 dynamic mechanical analyser (DMA). The atmosphere was air, the test was 3-point bending (dual cantilever mode). The temperature range was from 30 °C to 120 °C with a heating speed of 3 °C/min. The frequency of loading was 1 Hz. The storage modulus and the loss factor were registered.

Creep testing was also performed with the TA Instruments (USA) Q800 DMA instrument in creep time temperature superposition (TTS) mode. The main parameters are summarised in Table 3. The test temperature range covers the operational temperature range of the mould inserts entirely.

Shore D hardness tests were also performed with a H04.3150 hardness tester (Zwick GmbH & Co. KG, Germany). Tests were performed at ten locations both on the specimens and on the mould inserts. We measured Shore D hardness at the back of the mould inserts (opposite the cavity surface) in order to avoid damaging the cavity surface before injection moulding. The hardness of the mould inserts was measured before the injection moulding series.

2.3. The comprehensive state monitoring of mould inserts

Our comprehensive state monitoring system was already presented in depth in [32,33]. Fig. 1 shows the test mould. The dimensions of the moulded plate were 65 × 55 × 2 mm, while the overall dimensions of the insert were 75 × 65 × 15 mm. The cavity was filled through a 1 mm thick edge gate. The state monitoring system consists of the strain measurement of mould inserts by two strain gauges (KMT-LIAS-06-3-350-5EL). One gauge is placed near the gate while the other is placed at the end of the flow length. Strain data were collected with a Spider 8 unit (Hottinger Baldwin Messtechnik GmbH, Austria). Temperature was measured with a Heraeus M222 Pt100 thermocouple (Heraeus Holding GmbH, Germany) with an Ahlborn Almemo 8990–6 data collector unit (Ahlborn Mess- und Regelungstechnik GmbH, Germany). A cyanoacrylate adhesive, 3 M Scotch Weld Plastic and Rubber Instant Adhesive PR100 (3 M Company, USA), was used to fix the gauges and the thermocouple.

Table 3
Parameters of DMA creep TTS testing.

Parameters used	Unit	Typical value
Bending stress	MPa	5
Furnace time	min	10
Creep time	min	30
Recovery	min	30
Minimum temperature	°C	30
Maximum temperature	°C	90
Temperature increment	°C	5
Atmosphere	Air	

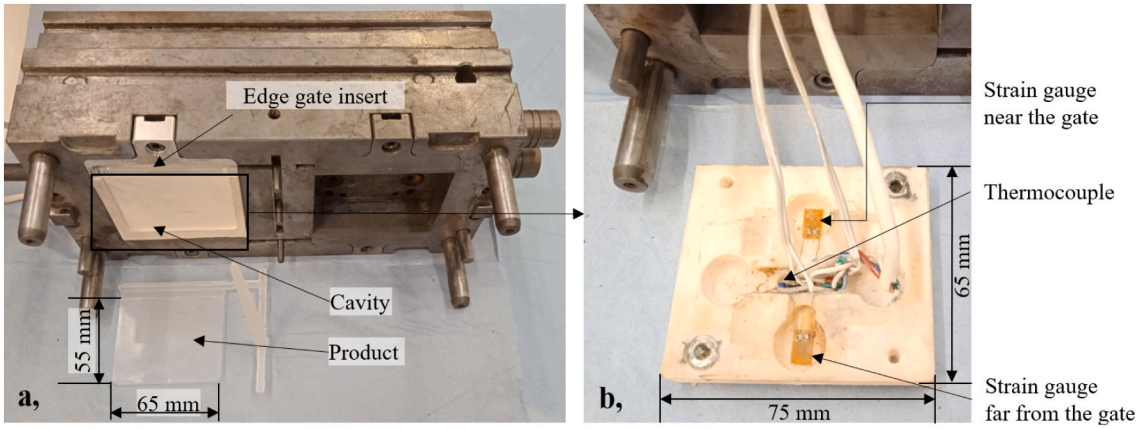

Fig. 1. The complete test mould and the injection moulded product a), the moving side insert with the strain gauges and the thermocouple b).

2.3.1. The injection moulding of samples

The injection moulded material was Tipplen H145F polypropylene homopolymer (MOL Group Plc., Hungary). It has a low recommended processing temperature range (190–235 °C) and an outstanding melt flow rate (MFR) value (29 g/10 min at 230 °C and 2.16 kg) which make it suitable for injection moulding into polymeric moulds as the material can be processed at a low temperature and with low injection pressure.

An Arburg Allrounder Advance 270S 400–170 (ARBURG GmbH, Germany) machine was used for injection moulding (screw diameter: 30 mm) the specimens. The processing parameters are listed in Table 4. A relatively low clamping force and injection pressure limit has to be set to protect the inserts from excessive mechanical loads. A long holding time and residual cooling time are necessary because the low thermal conductivity of the insert results in slow gate freeze and product solidification. Slow cooling also causes considerable product shrinkage, which has to be compensated for. A long delay time between the cycles is also essential to prevent the fast heating and early failure of the inserts.

We injection moulded 10 cycles at a constant holding pressure of 75 bar to characterise the stability and reproducibility of the injection moulding process. Following that, the holding pressure was gradually increased by 25 bar steps in every second cycle. We increased holding pressure from 50 bar to 300 bar to test the strength of the mould inserts. After the increasing holding pressure section, 10 cycles were injection moulded with a holding pressure of 125 bar, then an additional 10 cycles with 175 bar and finally 10 cycles with 225 bar.

2.3.2. 3D scanning of the mould inserts

The dimensional accuracy of the mould inserts was analysed with a GOM ATOS Core 5 M scanner (Carl Zeiss GOM Metrology GmbH, Germany). Mould inserts were scanned after irradiation and were compared with the nominal dimensions. The theoretical resolution of scanning is 0.01 mm.

Table 4
Parameters of injection moulding.

Processing parameters	Unit	Value
Clamping force	t	5
Injection rate	cm^3/s	15
Injection pressure limit	bar	500
Holding time	s	15
Residual cooling time	s	30
Dose volume	cm^3	40
Cycle time (from mould closing to mould opening)	s	~56.6
Overall cycle time (delay time included)	s	300
Switchover point	cm^3	26
Holding pressure	bar	50 to 300

3. Results and discussion

3.1. Specimen testing

3.1.1. Dynamic mechanical analysis

We performed a range of material tests to analyse the effect of irradiation on the parts made from VeroWhite. First, the storage modulus and the loss factor (tanδ) were determined by conventional DMA. The storage modulus-temperature curves characterise the temperature dependence of the material stiffness while the loss factor-temperature curves characterise the glass transition temperature of the material. The storage modulus and the loss factor (tanδ) is presented in Fig. 2. As the absorbed dose increased, the decrease in storage modulus shifted towards the higher temperature region. It proves that the stiffness of the material can be retained at higher temperatures with high enough doses of gamma irradiation. A saturation can also be observed as there is no significant difference between the specimens irradiated by the 150–200 kGy doses. It can indicate that an optimal irradiation dose exists that is low enough to prevent degradation, yet the storage modulus can be kept at a suitably high temperature. Similar tendencies apply to the loss factor as the maximum points of the curves shift towards the higher temperature region. The glass transition temperature is proportional to the maximum points of the loss factor. These maximum points were: 70.8 °C, 76.9 °C, 79.8 °C, 81.4 °C and 81.6 °C for the absorbed doses of 0, 50, 100, 150 and 200 kGy, respectively. The approximately 10 °C increase in the glass transition temperature as a result of irradiation by 200 kGy is beneficial for the resistance of the material against the heat load.

3.1.2. Creep tests

Creeping predominantly influences the operational deformation of the mould inserts, especially at elevated temperatures. The material's tendency to creep can be characterised by DMA in creep time temperature superposition (TTS) mode. Creep compliance (J) measures the deformation coming from creep and it can be calculated from the time-dependent flexural strain (ε_{fl}) and the pre-set flexural stress (σ_0), according to Eq. (1). Higher creep compliance indicates increased deformations coming from creep.

$$J(t) = \frac{\varepsilon_{fl}(t)}{\sigma_0} \tag{1}$$

Fig. 3 shows creep compliance for the specimens with different absorbed doses. The 0 kGy (untreated) specimen showed the highest creep compliance at nearly all the analysed temperatures, meaning that deformations coming from creep are excessive. However, as the dose rate increased, creep compliance dropped at each temperature indicating increased resistance against creep. The specimens irradiated with

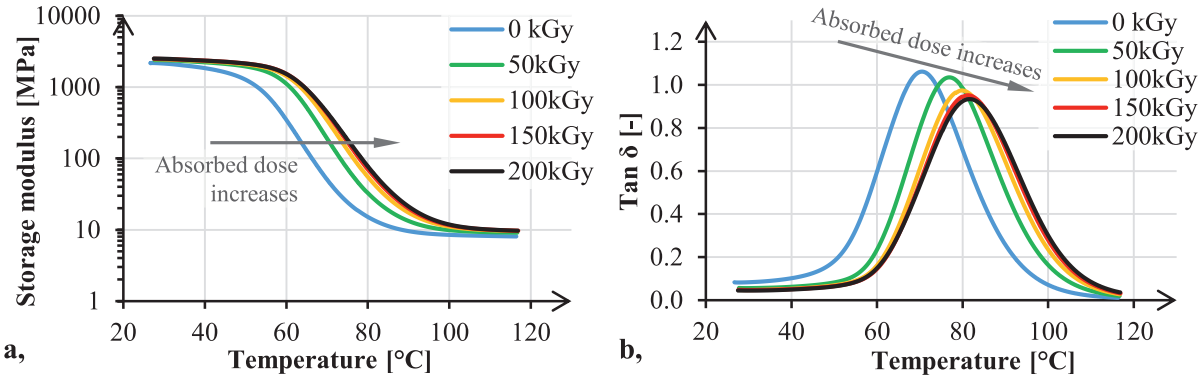

Fig. 2. Storage modulus (a) and loss factor (b) of VeroWhite specimens with different absorbed doses.

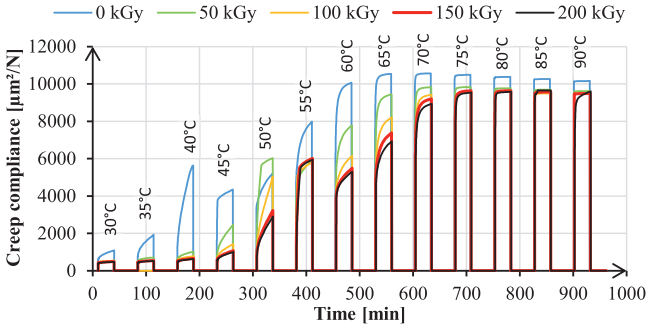

Fig. 3. Creep compliance of VeroWhite specimens with different irradiation doses at different temperatures.

200 kGy showed typically less than half the creep compliance than that of the 0 kGy specimens in the 30 °C to 65 °C temperature range. It is of significant practical relevance because that is the typical operational temperature range of the injection mould inserts. Above the optimal irradiation dose, mechanical properties do not improve. There is no significant difference in creep compliance between the specimens irradiated with 150 kGy and 200 kGy.

Maximal clamp (crosshead) displacements also prove that the irradiated specimens show higher stiffness. As the irradiation dose increased, the maximal clamp displacements fell almost throughout the entire analysed temperature region, which covers the operational temperature range. The results are presented in Fig. 4.

3.1.3. Surface hardness

Hardness is suitable for characterising the degree of cross-linking in the material as cross-linking increases hardness. Hardness was also measured on rectangular 4 × 10 × 59 mm specimens, in 10 points each, and average Shore D hardness and standard deviation were calculated (Fig. 5). The average hardness of the untreated (0 kGy) specimen was 81.3, which rose to the range of 84.4–85.1 for the irradiated specimens. The low standard deviation indicates that the entire specimen geometry shows relatively even hardness. The increase in hardness is an indication of the post-curing and cross-linking caused by the gamma irradiation. Hardness shows no significant variation by dose.

3.1.4. Mould insert hardness and dimensional accuracy

The mould inserts were also tested for hardness at the back (opposite the cavity surface). Hardness was also measured in 10 points overall, covering the entire back surface. Hardness measurements were carried out to characterise the increase in the crosslink density caused by the irradiation. The increase in the surface hardness is the direct result of the increase in the crosslink density. The measurement locations, and average hardness and the standard deviation of hardness for the different absorbed doses are shown in Fig. 6. Irradiated injection mould inserts and DMA specimens had similar hardness. It proves that high-energy gamma radiation can easily post-cure the entire cross-section of the insert. Therefore, high-energy gamma radiation is an effective tool to post-cure bigger and more complicated geometries not just rectangular DMA specimens.

3.2. Dimensional stability of the inserts

We 3D scanned the mould inserts before injection moulding to check the dimensional accuracy of printing and to analyse the effect of irradiation on the warpage of the inserts (Fig. 7). The untreated mould insert shows the best dimensional accuracy as the maximum size deviation is only +0.06 mm at the corner points of the insert. As the irradiation dose increased, so did warpage at the corner points. For the insert irradiated

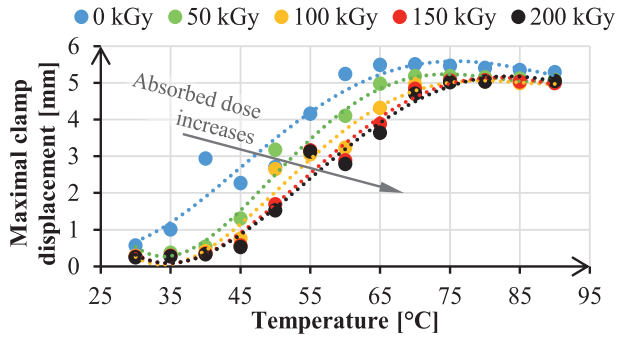

Fig. 4. Maximal clamp displacements of the bending tests of specimens irradiated by different doses.

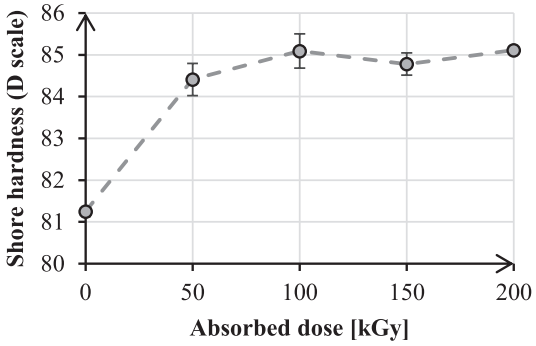

Fig. 5. Shore D hardness of VeroWhite specimens with different irradiation doses.

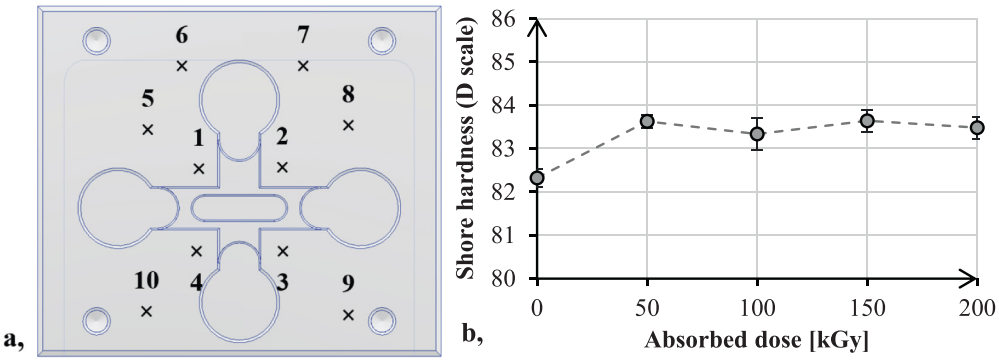

Fig. 6. Shore D hardness measurement locations of the printed mould inserts a) and the measured average hardness values with the standard deviations b).

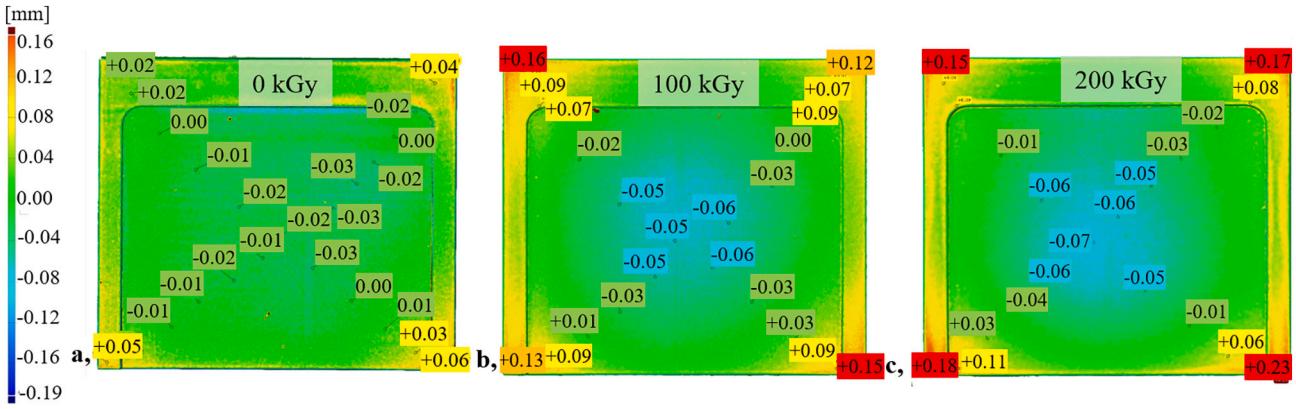

Fig. 7. 3D scanning of the printed mould inserts: 0 kGy a), 100 kGy b), 200 kGy c). The dimensions are in mm.

with 100 kGy, the maximum size deviation was +0.16 mm, which further increased to +0.23 mm for the insert irradiated with 200 kGy. The PolyJet™ technology has outstanding dimensionally accuracy but is also influenced by post-curing. Warpage at the outer corners of the inserts has to be kept as low as possible so the planarity of the mould parting plane can be preserved and the clamping force is transmitted uniformly. 3D scanning reinforced the expectation that ionizing radiation–induced post-curing causes warpage. However, dimensional

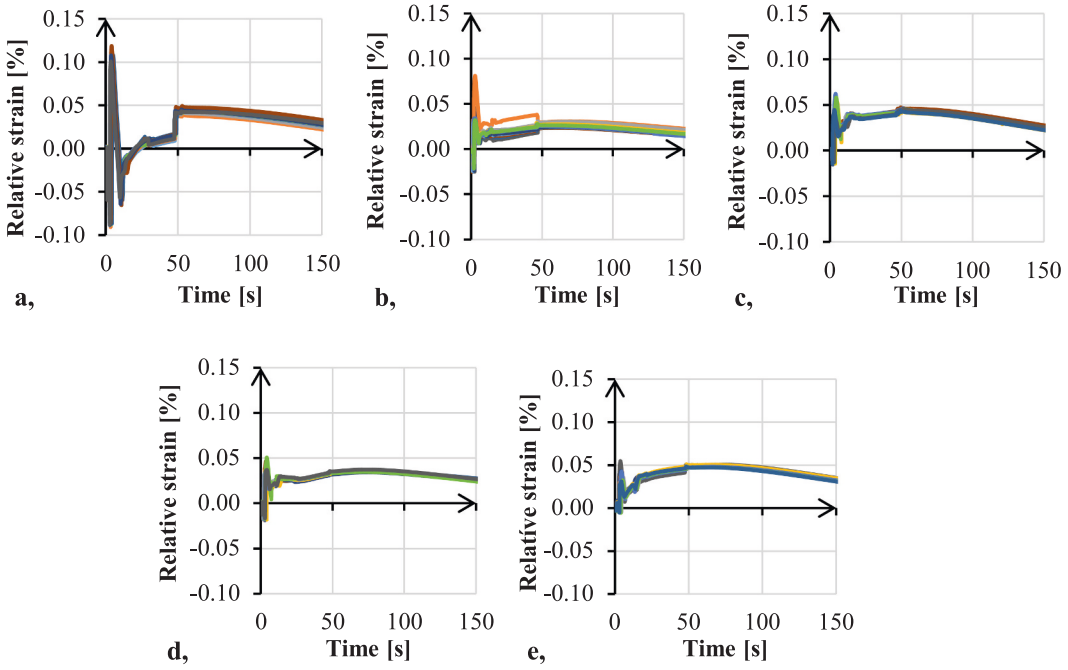

Fig. 8. The near-gate operational deformation of the untreated insert (a) and inserts irradiated with 50 kGy (b), 100 kGy (c), 150 kGy (d) and 200 kGy (e), injection moulded with a holding pressure of 75 bar.

deviation is well within the acceptable range and does not influence the applicability of the mould inserts fundamentally. These deviations still allow the mould inserts to be used because the cavity surface remains at nearly nominal dimension.

3.3. Injection moulding tests

3.3.1. Injection moulding with a constant holding pressure of 75 bar

After 3D scanning the inserts, injection moulding trials were run. 10 cycles were injection moulded with a constant holding pressure of 75 bar. The untreated mould insert showed significantly higher deformations (a maximum of ~0.12 %) compared to all of the irradiated inserts (~0.05 to 0.08 %). There were no significant differences between the deformations of the irradiated inserts, so a suitably low irradiation dose can decrease deformation compared to the untreated insert. These results reinforce that irradiation can reduce operational deformations significantly, which is beneficial for the applicability of MJ printed injection mould inserts (Fig. 8).

3.3.2. Injection moulding with increasing holding pressure

After injection moulding 10 cycles with a constant holding pressure of 75 bar, we increased holding pressure by 25 bar in every second cycle, from 50 bar to 300 bar to determine the pressure limit for applicability. Fig. 9 shows the operational deformations of the mould inserts. The untreated insert showed the highest deformations while the irradiated inserts exhibited gradually decreasing deformations, depending on the radiation dose. The mould insert irradiated with 200 kGy showed the lowest deformations, which is excellent proof that irradiation can increase the stiffness of the inserts effectively. Increasing holding pressure necessarily resulted in larger deformations for all analysed inserts. The shapes of the strain curves also vary greatly depending on the absorbed dose, especially with the highest, 300 bar holding pressure (indicated by the black curves in Fig. 9). In the case of the untreated insert, strain rose sharply during the entire injection moulding cycle and exceeded 1 % by mould opening. Relative strain only dropped because the cycle ended, the mould was opened and the part was ejected. On the other hand, the relative strain curves of the irradiated inserts all show a well-defined local maximum point in the holding phase and a nearly constant plateau can be observed in residual cooling time until mould opening. It indicates that the strain of the irradiated inserts stabilise even at the highest holding pressure of 300 bar. It is outstanding because the stabilised mould insert deformations result in more stable and repeatable production. That can be attributed to irradiation, which lowers creep compliance and increases the glass transition temperature, as the injection moulding parameters were identical.

3.3.3. Repeatability tests with different holding pressures

After the increasing holding pressure series, the injection moulding series was continued by cycles moulded at constant holding pressures to analyse the repeatability of the process. 10 cycles were injection moulded with a holding pressure of 125 bar then 10 cycles with 175 bar and 10 cycles with 225 bar, and all the mould inserts endured the load without visible failure. Fig. 10 shows the operational strain of the mould inserts injection moulded with a holding pressure of 225 bar. All the inserts showed acceptable stability of the technology, as the strain curves show little scatter. As the irradiation dose increased, maximum strain (occurring in the early holding phase) gradually decreased. Maximum relative strain was ~0.5 % for the untreated insert, which fell to 0.37 % for the insert irradiated with 200 kGy. It is desirable from a technological point of view because mould deformation impacts not just the lifetime of the mould but product quality and dimensional accuracy as well.

Fig. 11 shows the maximum relative strains at different irradiation doses and holding pressures. Increasing holding pressures resulted in increasing relative strain maximums. As the irradiation doses increased, the maximum relative strains fell for nearly all analysed holding pressures (indicated by the dotted lines). It means that ionizing irradiation is an effective tool to decrease the operational deformations of the mould inserts. The low standard deviations of the maximum relative strains indicate the stability and reproducibility of the technology.

Fig. 12 shows the correlations between maximum cavity pressure and maximum relative strain in each cycle. As the irradiation dose increased, maximum relative strain fell. Cross-linked materials exhibit instantaneous elastic deformation to the pressure load below T_g, which is the main reason for their application as injection moulds. Instantaneous elastic deformation below T_g means that a linear correlation can be assumed between maximum cavity pressure and maximum relative strain with satisfactory coefficients of determination (R^2). If deviations

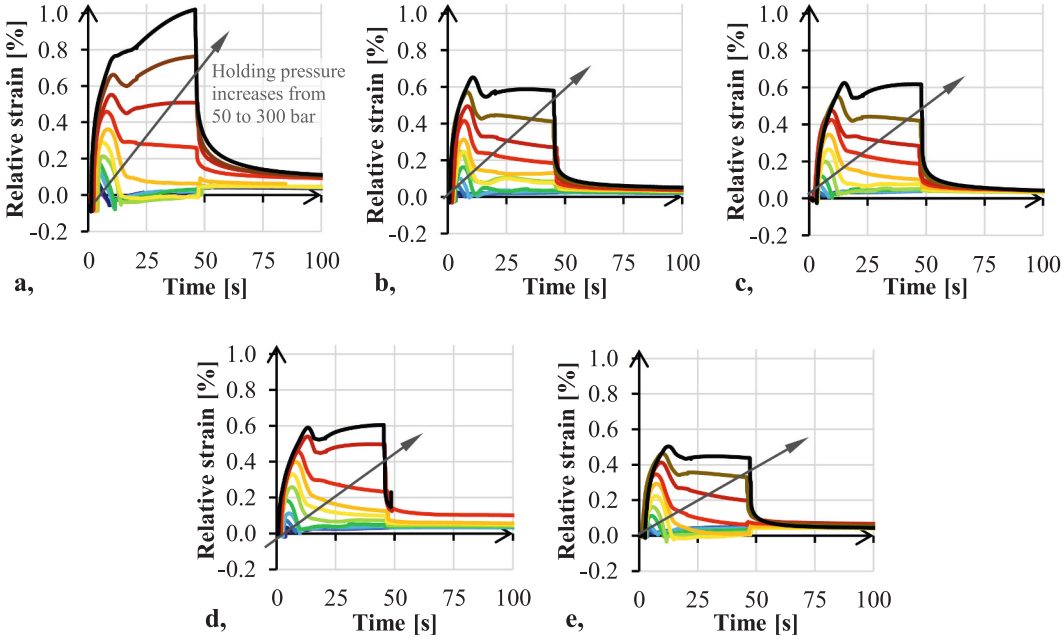

Fig. 9. Near-gate operational deformation of the untreated inserts (a) and inserts irradiated with 50 kGy (b), 100 kGy (c), 150 kGy (d) and 200 kGy (e), injection moulded with different holding pressures.

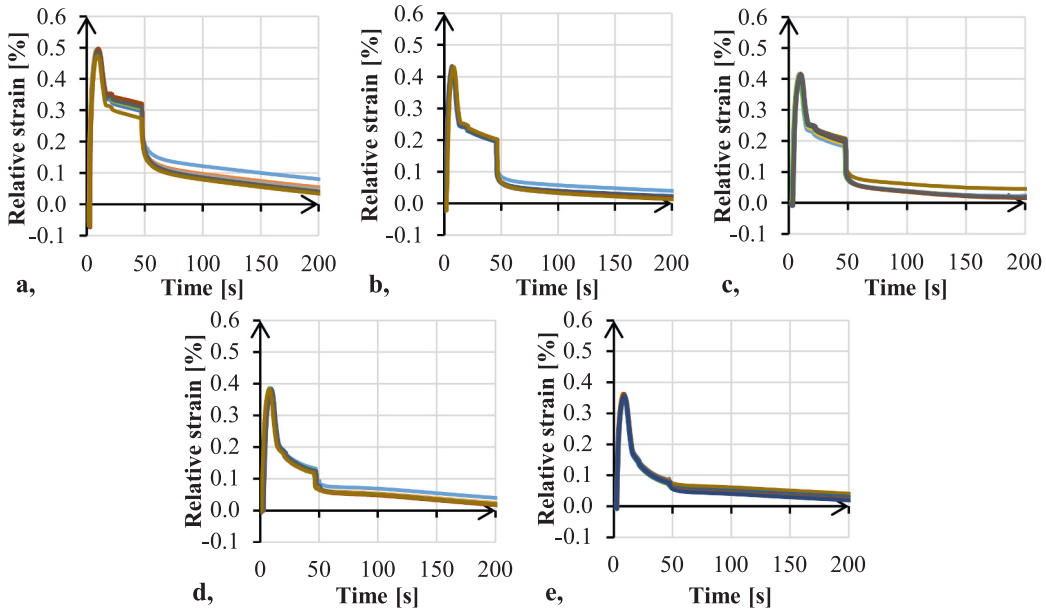

Fig. 10. The operational deformation of the injection mould inserts irradiated with different doses: 0 kGy a), 50 kGy b), 100 kGy c), 150 kGy d) and 200 kGy e), injection moulded with a holding pressure of 225 bar.

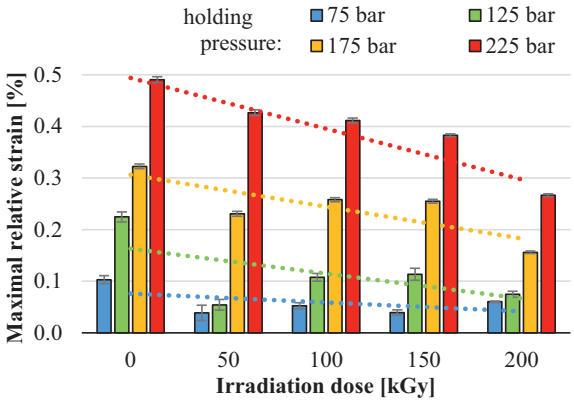

Fig. 11. The maximal relative strain as function of the irradiation dose measured at different holding pressure.

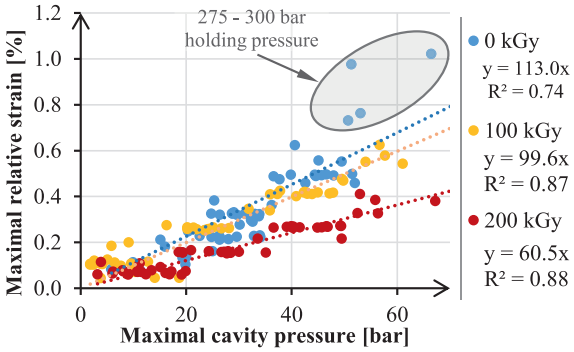

Fig. 12. Correlational diagram of maximum cavity pressure and maximum relative strain for the inserts irradiated with different doses.

occur from the linearity below T_g, they can be attributed to the excessive pressure load causing damage to the cross-linked structure. The effect of this excessive pressure load can be best observed at holding pressures of 275 and 300 bar, as these points show higher divergence from the linear correlation in the case of the untreated (0 kGy) insert. Fig. 9a) shows the progressive growth of strain for higher holding pressures. These deviating points are also highlighted in Fig. 12. The coefficients of the fitted lines clearly show a decreasing tendency with the increase of irradiation dose, which expresses mathematically the stiffness change of the mould inserts.

Table 5 presents the coefficients for linear fitting, together with the coefficients of determination for each irradiation dose level. The slope of the fitted lines show a decreasing tendency as the irradiation dose increases, which proves the stiffness-enhancing effect of radiation on the MJ printed mould inserts. There is a clear difference between the coefficients of linear fitting of the untreated insert, the inserts irradiated with 50, 100, and 150 kGy, and the insert irradiated with 200 kGy. These results prove that dose rate has a profound effect on the stiffness of the mould inserts. The coefficients of determination are also in the satisfactory range, confirming the suitability of the fitted correlational curve.

3.3.4. *Operational temperature of mould inserts*

Temperature was measured at the back of the insert with a thermocouple (Fig. 13 for 200 kGy). All inserts had a similar temperature–time curve, which means that irradiation did not have a significant effect on the thermal state of the mould inserts. Temperature rose more slowly when holding pressure was a constant 75 bar because the initial heating of the insert already occurred and the low holding pressure resulted in a relatively low heat transfer coefficient between the melt and the cavity wall. After the 10 cycles with a constant holding pressure of 75 bar, the temperature rose faster again as the increasing holding pressure (from 50 bar to 300 bar) resulted in better heat transfer

Table 5
Correlational coefficients between maximum cavity pressures and the corresponding maximum relative strains.

Dose [kGy]	Coefficients of linear fitting [1/bar]	Coefficients of determination [–]
0	113.0	0.74
50	99.4	0.76
100	99.6	0.87
150	96.1	0.76
200	60.5	0.88

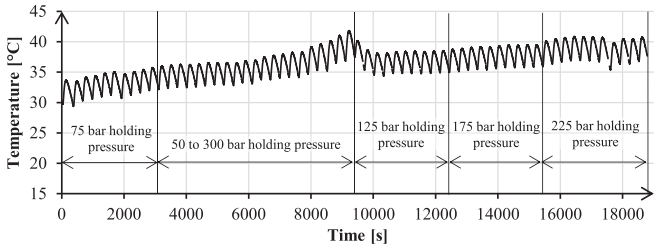

Fig. 13. Results of the thermocouple temperature measurement (insert irradiated with 200 kGy).

between the melt and the cavity wall. Higher holding pressure also results in the overfilling of the cavity, which means additional heat load on the insert. Maximum temperature occurred in the cycle with the highest, 300 bar holding pressure (~41 °C). Due to the bad thermal conductivity of the material (Table 2) the surface temperature of the cavity can be well above the glass transition range [32]. As holding pressure was lowered from 300 bar to 125 bar, the temperature also dropped due to the worse heat transfer from the melt to the insert. During the 10 cycles with a holding pressure of 125 bar, temperature rose slowly. During the 175 bar and later the 225 bar constant holding pressure section (10 cycles each) temperature slowly increased to approximately 40 °C again. Due to these relatively high temperatures even at the back of the insert, it is essential to increase the glass transition temperature of the insert material as much as possible. If the glass transition temperature is increased, a larger volume of the insert can be kept below T_g therefore stiffness can be retained.

3.3.5. *Mould insert dimensional accuracy after injection moulding*

Residual deformations of the mould inserts were also measured by 3D scanning (Fig. 14) for the untreated insert (0 kGy) and the insert irradiated by 200 kGy. The untreated insert shows significant residual deformations around the outer surface forming the parting plane of the mould. There are several deep slots around the cavity edge (−0.75 to +0.73 mm deep), which are caused by the combination of the repeated heat and pressure load of the injected melt, and the clamping force transmitted through the parting plane. The 2 mm deep side walls of the cavity also suffered significant residual deformations all around the circumference. The lower, flat surface of the cavity (65 × 55 mm) also exhibits observable residual deformations above the four slots of the strain gauges and the sensor cables (varying between −0.20 and − 0.31 mm). On the other hand, the dimensions of the cavity surface of the insert irradiated with 200 kGy almost remained its nominal dimensions, only the filleted corners show considerable deformation (+0.25 to +0.27 mm). Segments of the parting plane, especially around the upper right corner show significant deviations from the nominal geometry (−0.80 to +0.08 mm). These deviations in the parting plane can be attributed to the relatively large number of cycles injection moulded with higher holding pressures which results in the overfilling of the cavity. The additional injected material needs free space, which results in gradual mould opening and the occurrence of flash in the parting plane. Flash damages the mould surface, which results in the residual deformation described earlier. The pressure load does not deform the lower (65 × 55 mm) surface of the cavity because of the enhanced stiffness of the post-cured insert, irradiated with 200 kGy. In contrast, overfilling in the case of higher holding pressures causes damaged cavity sidewalls and residual deformations above the slots in the untreated (0 kGy) insert. The 3D scanning results of the untreated (0 kGy) insert and the insert irradiated with 200 kGy clearly show that ionizing radiation decreases the operational deformation of the MJ printed mould inserts, which significantly enhances their applicability. The considerable residual deformation of the untreated (0 kGy) insert also explains the deviation from the linear correlation between maximum relative strain and maximum cavity pressure (Fig. 12). Residual deformations prove that holding pressure exceeded the range where only instantaneous elastic deformation occurs.

4. Conclusions

In this article, we presented the effects of high-energy gamma radiation on the storage modulus, the loss factor and the Shore D hardness of VeroWhite specimens. Injection moulding tests were also performed and the operational deformation of material jetting printed mould inserts decreased considerably with increasing irradiation dose.

First, we carried out material testing to analyse the effects of radiation on the mechanical properties of parts made from VeroWhite resin. The storage modulus and glass transition temperature of the specimens irradiated with different doses (0, 50, 100, 150 and 200 kGy) were determined by conventional DMA. The decrease in the storage modulus and the maximum points of the loss factor shifted towards higher temperatures. The maximum point of the loss factor measured on the untreated (0 kGy) specimen was at 70.8 °C that grew to 81.6 °C for the specimen irradiated with 200 kGy which is a 15 % increase. It is a clear indication that the stiffness of the material is retained even at elevated temperatures, which is highly desirable for an injection mould insert. Alongside conventional DMA, DMA creep testing was also carried out in creep time–temperature superposition mode. Higher irradiation doses resulted in significantly lower creep compliance at all the analysed temperatures (30 to 90 °C). The maximal creep compliance at 40 °C measured on the untreated (0 kGy) specimen was 5629 $\mu m^2/N$ that fell to 621 $\mu m^2/N$ for the specimen irradiated with 200 kGy dose. It is a 89 % decrease which is also an excellent result because creep has a dominant

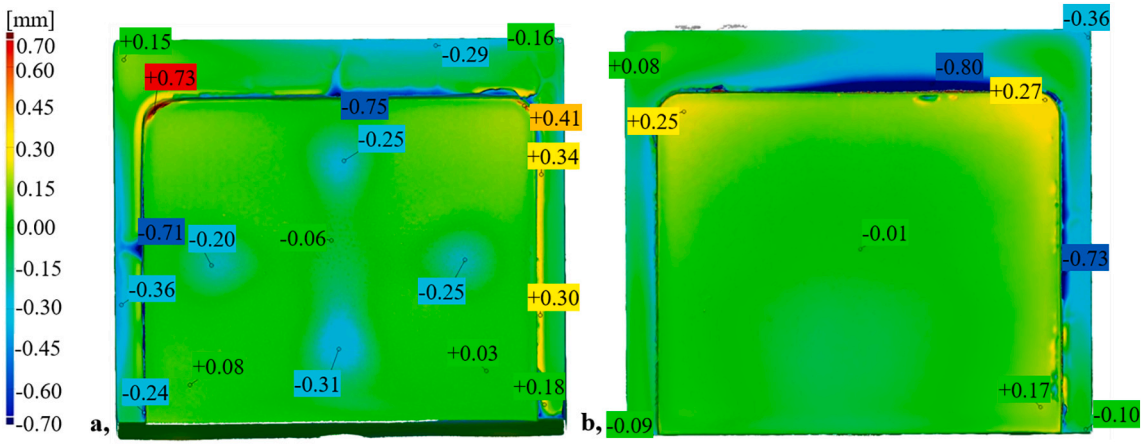

Fig. 14. Residual deformations of the mould inserts: untreated (0 kGy) a) and irradiated with 200 kGy b). The dimensions are in mm.

role in mould insert deformation. Clamp displacements also proved favourable because as the irradiation dose increased, maximum clamp displacements decreased, which means that the stiffness of the material improved. Shore D hardness was measured on both the DMA bending test specimens and the printed mould inserts. Shore D hardness increased from 81.3 measured on the untreated (0 kGy) specimen to 85.1 measured on the specimen irradiated with 200 kGy which means a 4.7 % increase. Both geometries had similar hardness, which means that high-energy radiation can induce cross-linking even in significantly thicker mould inserts, and so post-curing by radiation is not limited to smaller geometries.

After the hardness tests, injection moulding trials were run with the different inserts, irradiated with 0, 50, 100, 150 and 200 kGy. Operational strains were measured with strain gauges. During the injection moulding trials, repeatability tests were performed with constant holding pressure (75 bar). The effect of irradiation was clearly shown on the operational deformation of the mould inserts. The untreated insert showed the highest strains (~0.11–0.13 %), which gradually fell to ~0.04–0.05 % in the case of the insert irradiated with 200 kGy. After the 75 bar constant holding pressure section, holding pressure was gradually increased from 50 bar to 300 bar and the strains of the different inserts were measured and compared. The deformation of the inserts fell as the irradiation dose increased. That was especially evident in the case of the highest holding pressure of 300 bar. All irradiated inserts showed significantly lower deformations than the untreated insert. The maximum deformation for the untreated insert was above 1 %, which occurred right before mould opening, as deformations rose sharply even during residual cooling time. On the other hand, maximum deformations for the irradiated inserts were around or below 0.6 % and maximum strain occurred in the holding phase. During residual cooling time, the strains stabilised, which increases the lifetime of the inserts. The comparison of the maximum strains measured during the repeatability tests of inserts injection moulded with a holding pressure of 75, 125, 175 and 225 bar indicated that increasing irradiation dose resulted in decreasing maximum deformation.

This study presented the beneficial effect of gamma radiation–induced post-curing (cross-linking) on the glass transition temperature, creep compliance and hardness of specimens printed by material jetting from VeroWhite resin. Hardness tests of the printed mould inserts proved that larger geometries can also be properly post-cured by gamma radiation. Injection moulding trials proved that irradiation reduced operational deformations significantly, especially with higher holding pressures, where creep becomes more dominant. Gamma radiation is an effective tool to enhance the applicability of material jetting printed mould inserts, made from UV curable resins.

CRediT authorship contribution statement

Szabolcs Krizsma: Writing – original draft, Visualization, Validation, Investigation, Formal analysis, Data curation. **László Mészáros:** Writing – review & editing, Supervision, Methodology, Conceptualization. **Norbert Krisztián Kovács:** Writing – review & editing, Supervision, Methodology, Conceptualization. **András Suplicz:** Writing – review & editing, Writing – original draft, Supervision, Resources, Methodology, Funding acquisition, Conceptualization.

Funding

This work was supported by the National Research, Development and Innovation Office, Hungary (OTKA FK134336). Project no. RRF-2.3.1-21-2022-00009, titled National Laboratory for Renewable Energy has been implemented with the support provided by the Recovery and Resilience Facility of the European Union within the framework of Programme Széchenyi Plan Plus. This research was funded by the Horizon Europe Framework Programme and the call HORIZON-WIDERA-2021-ACCESS-03, under the grant agreement for project 101079051 – IPPT_TWINN. The authors also extend their acknowledgment to the International Atomic Energy Agency (IAEA) for financial support under the umbrella of CRP (Coordinated Research Project).

Declaration of competing interest

The authors declare that they have no known competing financial interests or personal relationships that could have appeared to influence the work reported in this paper.

Acknowledgements

We wish to thank ARBURG HUNGÁRIA KFT. for the ARBURG Allrounder injection moulding machine, and TOOL-TEMP HUNGÁRIA KFT., LENZKES GMBH and PIOVAN HUNGARY KFT. for the accessories.

References

[1] Alkentar R, Mankovits T. A study on the shape and dimensional accuracy of additively manufactured titanium lattice structures for orthopedic purposes. Periodica Polytechnica Mechanical Engineering 2022;66(4):336–43. https://doi.org/10.3311/PPme.20382.
[2] Zink B, Kovács NK, Kovács JG. Thermal analysis based method development for novel rapid tooling applications. Int Commun Heat Mass Transf 2019;108:104297. https://doi.org/10.1016/j.icheatmasstransfer.2019.104297.
[3] Mendible GA, Rulander JA, Johnston SP. Comparative study of rapid and conventional tooling for plastics injection molding. Rapid Prototyp J 2017;23(2):344–52. https://doi.org/10.1108/RPJ-01-2016-0013.
[4] A. Bagalkot, D. Pons, D Clucas, D. Symons: A methodology for setting the injection moulding process parameters for polymer rapid tooling inserts, Rapid Prototyp. J., 25(9), pp. 1493–1505, doi:https://doi.org/10.1108/RPJ-10-2017-0217.
[5] Simpson P, Zakula AD, Nelson J, Dworshak JK, Johnson EM, Ulven CA. Injection molding with an additive manufactured tool. Polym Eng Sci 2019;59:1911–8. https://doi.org/10.1002/pen.25192.
[6] Davoudinejad A, Khosravani MR, Pedersen DB, Tosello G. Influence of thermal ageing on the fracture and lifetime of additively manufactured mold inserts. Eng Fail Anal 2020;115:104694. https://doi.org/10.1016/j.engfailanal.2020.104694.
[7] Davoudinejad A, Bayat M, Pedersen DB, Zhang Y, Hattel JH, Tosello G. Experimental investigation and thermo-mechanical modelling for tool life evaluation of photopolymer additively manufactured mould inserts in different injection moulding conditions. Int J Adv Manuf Technol 2019;102:403–20. https://doi.org/10.1007/s00170-018-3163-7.
[8] A. Elkaseer, K. J. Chen, J. C. Janhsen, O. Refle, V. Hagenmeyer, S. G. Scholz: Material jetting for advanced applications: a state-of-the-art review, gaps and future directions, Additive Manufacturing, 60 Part A (2022), 103270, doi:https://doi.org/10.1016/j.addma.2022.103270.
[9] Russo C, Fernandez-Francos X, De la Flor S. Shape-memory actuators based on dual-curing thiol-acrylate-epoxy thermosets. Express Polymer Letters 2022;15(1):58–71. https://doi.org/10.3144/expresspolymlett.2021.7.
[10] Golhin AP, Strandlie A. Optical properties of tilted surfaces in material jetting. Optics & Laser Technology 2024;168:109992. https://doi.org/10.1016/j.optlastec.2023.109992.
[11] Golhin AP, Strandlie A. Appearance evaluation of digital materials in material jetting. Opt Lasers Eng 2023;168:107632. https://doi.org/10.1016/j.optlaseng.2023.107632.
[12] Golhin AP, Srivastava C, Strandlie A, Sole AS, Grammatikos S. Effects of accelerated aging on the appearance and mechanical performance of materials jetting products. Materials & Design 2023;228:111863. https://doi.org/10.1016/j.matdes.2023.111863.
[13] Bezek LB, Williams CB. Process-structure-property effects of ultraviolet curing in multi-material jetting additive manufacturing. Addit Manuf 2023;73:103640. https://doi.org/10.1016/j.addma.2023.103640.
[14] Samyn P, Bosmans J, Cosemans P. Influence of UV curing parameters for bio-based versus fossil-based acrylates in mechanical abrasion. Express Polymer Letters 2022;16(7):718–34. https://doi.org/10.3144/expresspolymlett.2022.53.
[15] Zhao P, He Y, Trindade GF, Baumers M, Irvine DJ, Hague RJM, et al. Modelling the influence of UV curing strategies for optimisation of inkjet based 3D printing. Materials and Design 2021;208:109889. https://doi.org/10.1016/j.matdes.2021.109889.
[16] Liang J, Francoeur M, Williams CB, Raeymaekers B. Curing characteristics of a photopolymer resin with dispersed glass microspheres in vat polymerization 3D printing. ACS Applied Polymer Materials 2023;5(11):9017–26. https://doi.org/10.1021/acsapm.3c01479.
[17] Bean RH, Nayyar G, Brown MK, Wen J, Fu Y, Winey KI, et al. Vat photopolymerization of poly(styrene-b-isoprene-b-styrene) triblock copolymers. Addit Manuf 2024;92:104391. https://doi.org/10.1016/j.addma.2024.104391.
[18] Rau DA, Bryant JS, Reynolds JP, Bortner MJ, Williams CB. A dual-cure approach for the ultraviolet-assisted material extrusion of highly loaded opaque suspensions. Addit Manuf 2023;72:103616. https://doi.org/10.1016/j.addma.2023.103616.

[19] Wen J, Bean RH, Nayyar G, Feller K, Scott PJ, Williams CB, et al. Vat photopolymerization of synthetic isoprene rubber latexes. ACS Applied Polymer Materials 2024;6(4):9017–26. https://doi.org/10.1021/acsapm.3c02604.
[20] Shaffer S, Yang K, Vargas J, Di Prima MA, Voit W. On reducing anisotropy in 3D printed polymers via ionizing radiation. Polymer 2014;55(23):5969–79. https://doi.org/10.1016/j.polymer.2014.07.054.
[21] Liu P, Zhu J, Cheng L, Liu X, Liu R. Curing and properties of urethane acrylates with different functionalities under electron-beam and ultraviolet irradiation. Prog Org Coat 2021;156:106252. https://doi.org/10.1016/j.porgcoat.2021.106252.
[22] Wu ZX, Li JW, Huang CJ, Huang RJ, Li LF. Effect of gamma irradiation on the mechanical behavior, thermal properties and structure of epoxy/glass-fiber composite. Journal of Nuclear Materials 2013;441(1–3):67–72. https://doi.org/10.1016/j.jnucmat.2013.05.041.
[23] Hoffman EN, Skidmore TE. Radiation effects on epoxy/carbon-fiber composite. Journal of Nuclear Materials 2009;392(2):371–8. https://doi.org/10.1016/j.jnucmat.2009.03.027.
[24] Idesaki A, Uechi H, Hakura Y, Kishi H. Effects of gamma-ray irradiation on a cyanate ester/epoxy resin. Radiation Physics and Chemistry 2014;98:1–6. https://doi.org/10.1016/j.radphyschem.2013.12.032.
[25] Diao F, Zhang Y, Liu Y, Fang J, Luan W. γ-Ray irradiation stability and damage mechanism of glycidyl amine epoxy resin. Nucl Instrum Methods Phys Res, Sect B 2016;383:227–33. https://doi.org/10.1016/j.nimb.2016.07.009.
[26] Jiao L, Zhao X, Guo Z, Chen Y, Wu Z, Yang Y, et al. Effect of γ irradiation on the properties of functionalized carbon-doped boron nitride reinforced epoxy resin composite. Polym Degrad Stab 2022;206:110167. https://doi.org/10.1016/j.polymdegradstab. 2022.110167.
[27] Chen K, Zhao X, Zhang F, Wu X, Huang W, Liu W, et al. Influence of gamma irradiation on the molecular dynamics and mechanical properties of epoxy resin. Polym Degrad Stab 2019;168:108940. https://doi.org/10.1016/j.polymdegradstab. 2019.108940.
[28] Wang L, Zhang F, Du S, Leng J. 4D printing of shape-changing structures based on IPN epoxy composites formed by UV post-curing and γ-ray radiation. Compos A: Appl Sci Manuf 2022;162:107146. https://doi.org/10.1016/j.compositesa.2022.107146.
[29] Jiao L, Wang Y, Wu Z, Shen H, Weng H, Chen H, et al. Effect of gamma and neutron irradiation on properties of boron nitride/epoxy resin composites. Polym Degrad Stab 2021;190:109643. https://doi.org/10.1016/j.polymdegradstab.2021.109643.
[30] Hassan MA, Dayo AQ, Zegaoui A, Derradji M, Hassane AM, Liu W-B, et al. Effect of gamma-rays on the thermal and mechanical properties of epoxy/tungsten boride composites. High Performance Polymers 2022;34(9):1058–68. https://doi.org/10.1177/09540083221105259.
[31] G. Szebényi, D. Faragó, Cs. Lámfalusi, R. Göbl: Interfacial adhesion improvement in carbon fiber/carbon nanotube reinforced hybrid composites by the application of a reactive hybrid resin initiated by gamma irradiation. Radiation Physics and Chemistry, 145, 2018, pp. 111–115, doi:https://doi.org/10.1016/j.radphyschem.2017.12.018.
[32] Krizsma Sz, Suplicz A. Comprehensive in-mould state monitoring of Material Jetting additively manufactured and machined aluminium injection moulds. Journal of Manufacturing Processes 2022;84:1298–309. https://doi.org/10.1016/j.jmapro.2022.10.070.
[33] Krizsma Sz, Suplicz A. Analysis of the applicability and state monitoring of material extrusion–printed acrylonitrile butadiene styrene injection mould inserts with different infill levels. Materials Today Communications 2023;35:106294. https://doi.org/10.1016/j.mtcomm.2023.106294.